Spin Delocalization in the Copper(I) Complexes of Bis(verdazyl) Diradicals

David J. R. Brook,*,† Vincent Lynch, Brenda Conklin, and Marye Anne Fox*,‡

Contribution from the Department of Chemistry and Biochemistry, University of Texas at Austin, Austin, Texas 78712, and Department of Chemistry and Biochemistry, University of Colorado, Boulder, Colorado 80309-0215

Received May 17, 1996. Revised Manuscript Received February 20, 1997[⊗]

Abstract: 1,1′,5,5′-tetramethyl-6,6′-dioxobis(verdazyl) (BVD) reacts with copper(I) halides in acetonitrile and copper(II) halides in methanol to give copper(I) coordination polymers of composition $[Cu_2X_2(BVD)]_x$. When X = Cl and X = Br, these polymers crystallize in orthorhombic unit cells with dimensions $a = 6.684(1)$ Å, $b = 12.524(3)$ Å, and $c = 8.717(2)$ Å (X = Cl) and $a = 12.680(2)$ Å, $b = 6.744(1)$ Å, and $c = 8.822(2)$ Å (X = Br). With X = I, powder diffraction indicates a monoclinic unit cell with dimensions $a = 12.669$ Å, $b = 8.461$ Å, $c = 7.679$ Å, and $\beta = 91.88°$, although poor crystal quality prevented a full structure determination. Magnetic susceptibility measurements taken on the three polymers indicate that the spins couple in one-dimensional chains with alternating exchange parameters: $J_1 = -190$ cm^{-1}, $J_2 = -116$ cm^{-1} (X = Cl); $J_1 = -200$ cm^{-1}, $J_2 = -110$ cm^{-1} (X = Br); and $J_1 = -271$ cm^{-1}, $J_2 = -200$ cm^{-1} (X = I). Variable temperature ESR measurements on the unstable monomeric complex resulting from reaction of BVD with $(CH_3O)_3PCuI$ indicate an interradical exchange parameter J of -230 cm^{-1}. ESR spectra of all three complexes show extremely broad, featureless lines as a result of very rapid spin−lattice relaxation. The reduction in exchange between the two halves of the bis(verdazyl) ligand upon coordination, and the unusual ESR properties, require a delocalized structure, with significant spin density on the copper atom. Variation of the auxiliary ligands on the copper atom allows tuning of the intramolecular exchange.

Introduction

The interaction between electrons in degenerate or near degenerate molecular orbitals is important in the study of many molecular and supramolecular properties. Although these interactions are relatively low in energy, they are vital for the accurate description of magnetic and electronic properties of molecules and materials. To allow for the rational design of magnetic and electronic systems, and to aid in the design of nanoscopic devices, it is important to be able to predict, if only roughly, the sign and magnitude of interelectronic exchange. Furthermore, to allow design flexibility, a tunable system of interactions is desirable. In magnetic systems, recent research has focused on transition metal complexes of organic radical ligands.[1,2] Such systems not only provide a probe for exchange interactions between unpaired electrons but in some instances have shown novel long range ordering effects.[1,3,4] Indeed, the only reported room temperature molecular magnet is believed to be a coordination polymer between vanadium(II) and a tetracyanoethylene radical anion.[5] Other metal−radical ligand systems that have been extensively studied include metal−semiquinone complexes,[6] coordination polymers based on bridging nitronyl or nitroxide ligands,[3] and polymers based on aromatic polynitroxides.[1] These studies have provided some remarkable examples of well-characterized materials showing novel magnetic ordering, but their complex three-dimensional interactions make a detailed understanding of the spin−spin interactions hard to achieve. In order to better understand metal−radical and radical−radical interactions, smaller and more easily analyzed systems must be studied.

We have previously reported the ESR and magnetic properties of the diradical 1,1′,5,5′-tetramethyl-6,6′-dioxobis(verdazyl) (BVD) and observed that the molecule has a singlet ground state with a thermally populated triplet lying 760 cm^{-1} above it.[7] BVD is ideally suited for radical coordination studies because

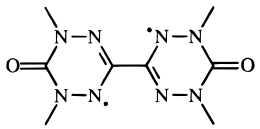

BVD

the radical−radical interaction is well-characterized. The diradical can chelate metals with relatively little geometric perturbation and consequently valuable information about the metal−radical and metal−metal interactions should be obtainable. Furthermore, BVD is a relatively rigid, chelating molecule analogous to bipyrimidine. Such molecules have been proposed as building blocks in the self-assembly of complex molecular structures,[8] and the prospect of employing this ligand as a key component of a carefully designed, discrete, self-assembling, polyradical system is intriguing. As an initial investigation of the coordination chemistry of this unusual diradical, we report here the synthesis and properties of the complexes of BVD with copper halides.

† University of Colorado.
‡ University of Texas at Austin.
[⊗] Abstract published in *Advance ACS Abstracts,* May 15, 1997.

(1) Iwamura, H.; Inoue, K.; Hayamizu, T. *Pure Appl. Chem.* **1996**, *68,* 243.
(2) Stumpf, H. O.; Ouahab, L.; Pei, Y.; Grandjean, D.; Kahn, O. *Science* **1993**, *261,* 447.
(3) Caneschi, A.; Gatteschi, D.; Sessoli, R.; Rey, P. *Acc. Chem. Res.* **1989**, *22,* 392.
(4) Kahn, O. *Molecular Magnetism;* VCH Publishers: New York, 1993.
(5) Manriquez, J. T.; Yee, G. T.; McLean, R. S.; Epstein, A. J.; Miller, J. S. *Science* **1991**, *252,* 1415.
(6) Pierpont, C. G.; Lange, C. W. *Prog. Inorg. Chem.* **1994**, *41,* 331.
(7) Brook, D. J. R.; Fox, H. H.; Lynch, V.; Fox, M. A. *J. Phys. Chem.* **1996**, 2066.
(8) Lehn, J. M. *Supramolecular Chemistry;* VCH: Weinheim, 1995.

S0002-7863(96)01675-7 CCC: $14.00

Results

BVD was synthesized from phosgene, methyl hydrazine, and glyoxal by literature methods.[9,10] Combination of chloroform and dichloromethane solutions of BVD with trimethyl phosphite−copper(I) iodide results in a change in the color of the solution from red-brown to a dark yellow-brown. Coordination of the ligand to copper is indicated by the shift of the carbonyl stretching frequency from 1690 cm^{-1} (free ligand in chloroform) to 1697 cm^{-1}. The absorption spectrum shows a peak at λ_{max} = 396 nm (ϵ = 4690 M^{-1} cm^{-1}) typical for a copper(I)−aromatic imine metal−ligand charge transfer absorption.[11] The expected shoulders in the spectrum at 420 and 500 nm cannot be resolved.

As a solution, the complex cannot be fully characterized as it is unstable and over a 24 h period deposits a black precipitate of $[Cu_2I_2(BVD)]_x$ with liberation of trimethyl phosphite. Nevertheless, the available spectral data are consistent with structures for the monomer **1** or an iodide-bridged oligomer such as **2**.

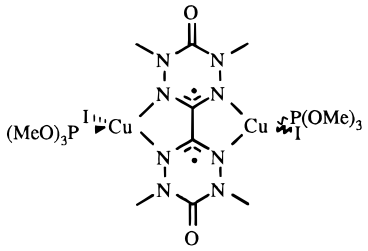

1

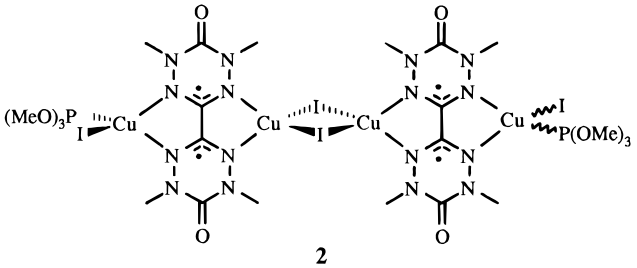

2

ESR spectra of many organic triplets can only observed in rigid matrices. In fluid solution, molecular tumbling rapidly modulates electronic dipole−dipole interactions, resulting in rapid spin−lattice relaxation and broadening of the ESR signal until it becomes undetectable.[12] The ESR spectra of BVD in frozen chloroform, before and after addition of $(CH_3O)_3PCuI$, are shown in Figure 1. At room temperature, chloroform solutions containing BVD and $(CH_3O)_3PCuI$ show only a narrow ESR signal which we assign to an oxidation contaminant of BVD present in samples of BVD in concentrations up to 1%.[7] Moreover, even when frozen (<200 K), the solution does not exhibit the anticipated triplet ESR spectrum; i.e., no fine structure arising from zero-field splitting can be observed. Instead, a very broad, indistinct resonance is observed as two shoulders in either side of the previously noted narrow signal. Repeated measurements at varying concentrations give the same broad, featureless spectrum at all temperatures, making it unlikely that this effect is caused by further aggregation.

The product of the ESR signal intensity (from double integration of the spectrum) and temperature falls with decreasing temperature, indicating a singlet ground state (Figure 2).

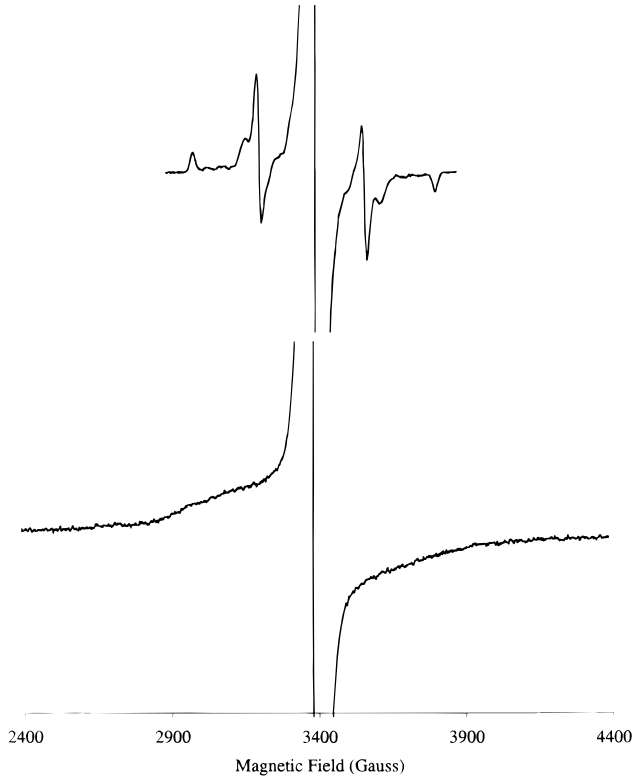

Figure 1. ESR spectra in frozen chloroform. The upper trace is from BVD and shows the fine structure arising from zero-field splitting. The lower trace is from a solution of BVD after addition of 2 equiv of $(CH_3O)_3PCuI$. Considerable broadening of the spectrum and loss of fine structure are apparent. The large central signal in both traces arises form a doublet impurity present in samples of BVD.

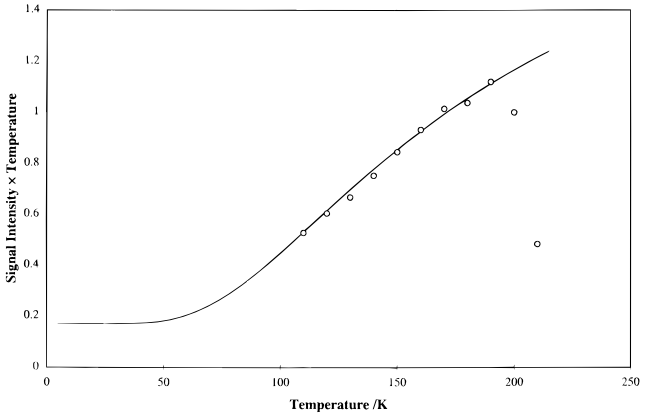

Figure 2. Doubly integrated ESR signal intensity × temperature vs temperature for the lower trace of Figure 1. The solid line is a best fit to the modified Bleaney−Bowers equation: $IT = \theta/(3 + e^{-J/k_BT}) + p$, with parameters J = 230 cm^{-1}, q = 8.1 K, and p = 0.17 K.

Curve fitting to the Bleaney−Bowers equation[13] gives a singlet−triplet separation J of −230 cm^{-1}. The broadening observed in the spectrum is too great to be explained by the additional hyperfine coupling to Cu and P, and this suggests a very fast spin−lattice relaxation time even in a rigid matrix. Because of the lack of detail in the spectrum, full spectral simulation to provide meaningful parameters is impossible; however, using the zero-field splitting parameters of BVD itself, and the hyperfine parameters from Kaim's copper(I)−bipyridine complex (*vide infra*), we can estimate the line width required to suppress the fine structure and produce a broad signal such as that observed. This method gives a very crude estimate of the

(9) Neugebauer, F. A.; Fischer, H. *Angew. Chem., Intl. Ed. Engl.* **1980**, *92*, 761.
(10) Neugebauer, F. A.; Fischer, H.; Siegel, R. *Chem. Ber.* **1988**, *121*, 815.
(11) Kutal, C. *Coord. Chem. Rev.* **1990**, *99*, 213.
(12) Weissman, S. I. *J. Chem. Phys.* **1958**, *29*, 1189.
(13) Bleaney, B.; Bowers, K. D. *Proc. R. Soc. London* **1952**, *A214*, 451.

Table 1. Unit Cell Dimensions for Copper(I) Complexes of BVD

	$[Cu_2Cl_2(BVD)]_x$	$[Cu_2Br_2(BVD)]_x$	$[Cu_2I_2(BVD)]_x$
crystal system	orthorhombic	orthorhombic	monoclinic
a (Å)	6.684(1)	12.608(2)	12.669(2)
b (Å)	12.524(3)	6.744(1)	8.461(2)
c (Å)	8.717(2)	8.822(2)	7.679(1)
β (deg)			91.88

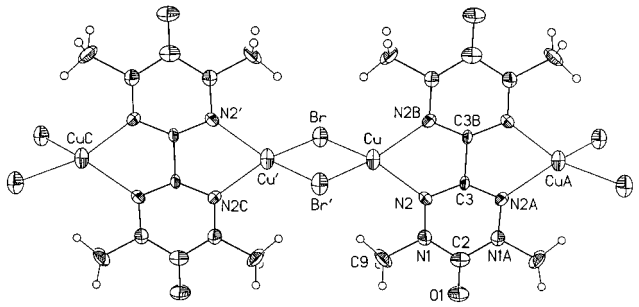

Figure 3. View of a portion of the polymeric $(Cu_2Br_2[BVD]_x)$ showing the atom labeling scheme. Thermal ellipsoids are scaled to the 30% probability level. The complex is extended parallel to *c*. The Cu_2Br_2 moiety lies around a position of symmetry 2/*m* at 1/2, 0, 0. Atoms labeled with a prime are related by $1 - x, -y, -z$. A crystallographic mirror plane of symmetry bisects the nearly planar BVD moiety passing through atoms O1, C2, C3, C3B, C2B, and O1B.

peak-to-peak line width, $\Delta B_{pp} \approx 120$ G, corresponding to a transverse relaxation time (T_2, *vide infra*) of approximately 5×10^{-10} s.

Upon combination of chloroform solutions of BVD with copper(I) halides in acetonitrile, a black microcrystalline precipitate with composition $[Cu_2X_2(BVD)]_x$ rapidly forms. The precipitate from the reaction with trimethyl phosphite−copper(I) iodide is identical in composition to that produced from copper(I) iodide. Combination of BVD with the copper(II) halides ($CuCl_2$ and $CuBr_2$) in methanol solution results in formation of analogous black microcrystalline precipitates: X-ray powder diffraction indicates that these precipitates are structurally identical to those obtained from the corresponding copper(I) halide. The powder patterns of the chloride and iodide complexes were indexed with the computer programs TREOR and VISSER.[14] Unit cell dimensions are given in Table 1 along with data for the bromide complex (*vide infra*). Careful layering of a methanolic solution of $CuBr_2$ upon a chloroform solution of BVD results, after diffusion of the layers together, in crystals of the $[Cu_2Br_2(BVD)]_x$ complex suitable for single-crystal X-ray diffraction study. Crystallographic data and the results of the structure refinement are summarized in Table 2. The structure of the material is polymeric, with copper atoms alternately bridged by halide ions and verdazyl diradicals (Figure 3). Atomic positional and equivalent isotropic thermal parameters are listed in Table 3, and bond lengths and angles for the non-hydrogen atoms are listed in Table 4. The chains pack in a herringbone arrangement, with each verdazyl π system overlapping a verdazyl ring of a neighboring chain (Figure 4), with a π stacking distance of 3.6 Å.

The unit cell of the chloride complex is isomorphic with the bromide and may thus be anticipated to have a very similar structure. The iodide, however, has a monoclinic rather than orthorhombic unit cell, suggesting a difference in packing brought about by the larger iodine atom. Although no crystals of the iodide complex suitable for single-crystal structure determination were obtained by interfacial precipitation, we infer that the iodine complex maintains a similar linear polymeric structure, but differs slightly in overall packing.

(14) Lasocha, W.; Lewinski, K. *PROSZKI: A System of Programs for Powder Diffraction Data Analysis*, v. 2.4; Krakow, Poland, 1994.

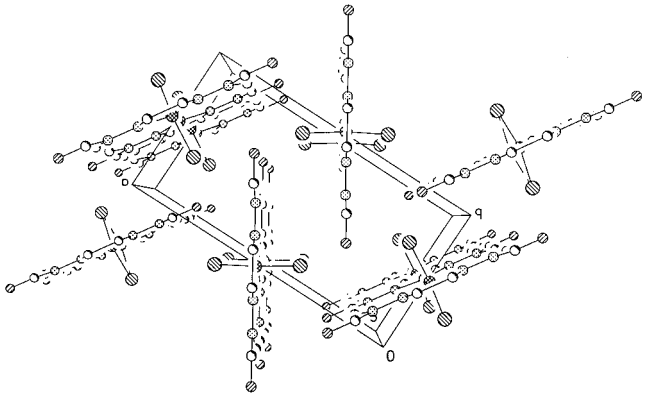

Figure 4. Unit cell packing diagram for $(Cu_2Br_2[BVD]_x)$. The view direction is along the *c* axis. A herringbone arrangement of layers of $(Cu_2Br_2[BVD]_x)$ is apparent in this orientation.

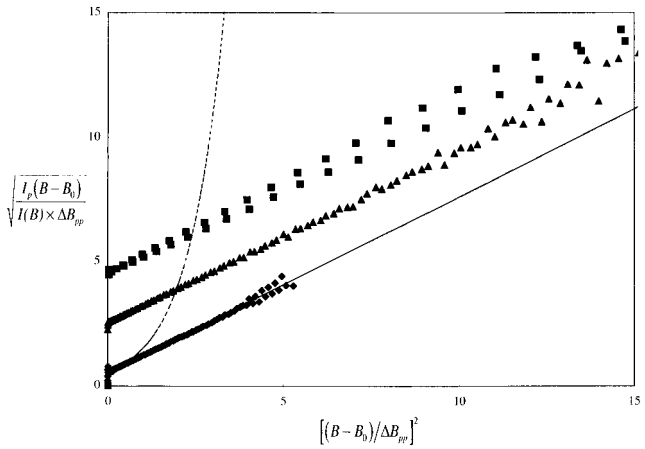

Figure 5. $[I_p(B - B_0)/\{I(B)\ \Delta B_{pp}\}]^{1/2}$ against $[(B - B_0)/\Delta B_{pp}]^2$ for $[Cu_2Cl_2(BVD)]_x$ (diamonds), $[Cu_2Br_2(BVD)]_x$ (triangles), and $[Cu_2I_2(BVD)]_x$ (squares). The plots for the bromide and iodide complexes are offset along the *y* axis to improve clarity. The solid and broken lines are the predicted behavior for Lorentzian and Gaussian line shapes, respectively. The plots indicate that the line shapes for these ESR spectra are Lorentzian over the width of the recorded spectrum.

ESR spectra of the crystalline complexes show extremely broad, featureless absorptions with peak-to-peak line widths on the order of several hundred gauss at room temperature ($g \approx 2.003$) and none of the *g* value anisotropy expected for a copper(II) species. For all three complexes, the line width increases with increasing temperature (Figure 6) and the signal intensity parallels the observed magnetic susceptibility. The line shape can be determined by plotting the function $[I_p(B - B_0)/\{I(B)\ \Delta B_{pp}\}]^{1/2}$ against $[(B - B_0)/\Delta B_{pp}]^2$, where I_p is the maximum (peak-to-baseline) height of the derivative line, $I(B)$ is the distance of the derivative curve from the baseline at field B, B_0 is the resonant field, and ΔB_{pp} is the peak-to-peak line width.[15] For a Lorentzian line shape, this plot should be linear: for a Gaussian line shape, this plot would curve upward. Figure 5 shows these plots for the three halide complexes: A line width that is essentially Lorentzian is observed in all cases, although there is some asymmetry in the line for the CuI complex.

The broad line width observed in the spectra of both the polymeric and the discrete species points to very fast relaxation times and an unusual electronic structure. Unfortunately, with such fast relaxation times, saturation of the ESR absorption

(15) Gatteschi, D.; Sessoli, R. *Magn. Reson. Rev.* **1990**, *15*, 1.

Table 2. Crystallographic Data[a] for $(Cu_2Br_2[(BVD)]_x)$

formula	$C_8H_{12}N_8O_2Cu_2Br_2$	no. of reflections measured	4894
fw	539.16	no. of unique reflections	708
a (Å)	12.680(2)	decay correction	0.9691−1.007
b (Å)	6.744(1)	R_{int} (F^2)	0.111
c (Å)	8.822(2)	μ (cm^{-1})	81.34
V (Å^3)	754.4(3)	crystal size (mm)	0.05 × 0.19 × 0.39
Z	2	transmission factor range	0.2271−0.5118
F(000)	520	$R_w(F^2)^b$	0.165
crystal system	orthorhombic	$R(F)^c$	0.0607
space group	*Pbam*	goodness of fit, S^d	1.065
T (°C)	−75	no. of parameters	57
2θ range (deg)	4−50	max $\lvert\Delta/\sigma\rvert$	<0.1
scan speed (deg/min) (1.6° ω scan)	5−12	min, max peaks (e^-/Å^3)	−0.55, 1.04
ρ_{calc}, g/cm^3	2.37		

[a] Data were collected on a Siemens P3 diffractometer, equipped with a Nicolet LT-2 low-temperature device and using graphite-monochromatized Mo Kα radiation (λ = 0.710 73 Å). Data were collected using ω scans with a scan range of 1.6° in ω. Lattice parameters were obtained from the least-squares refinement of 44 reflections with $9.9 < 2\theta < 15.9°$. [b] $R_w = \{\sum w(|F_o|^2 - |F_c|^2)^2/\sum w(|F_o|)^4\}^{1/2}$ where the weight, w, is defined as $w = 1/\{\sigma^2(|F_o|^2) + (0.1119P)^2\}$; $P = [(1/3)(\text{max of } (0 \text{ or } |F_o|^2) + (2/3)|F_c|^2]$. [c] The conventional R index based on F where the 404 observed reflections have $F_o > 4(\sigma(F_o))$. [d] $S = [\sum w(|F_o|^2 - |F_c|^2)^2/(n - p)]^{1/2}$, where n is the number of reflections and p is the number of refined parameters.

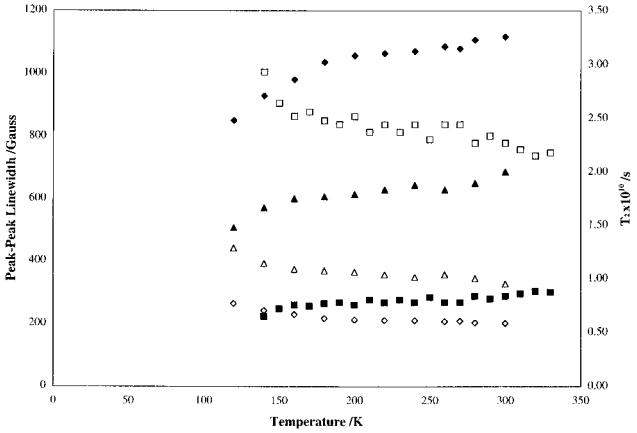

Figure 6. Temperature dependence of the peak-to-peak line width (ΔB_{pp}, filled symbols) and transverse relaxation time (T_2, open symbols) for $[Cu_2Cl_2(BVD)]_x$ (diamonds), $[Cu_2Br_2(BVD)]_x$ (triangles), and $[Cu_2I_2(BVD)]_x$ (squares). T_2 was calculated from the relationship $T_2 = (2/\sqrt{3})(1/\gamma\Delta B_{pp})$ where γ is the magnetogyric ratio for the electron.

Table 3. Fractional Coordinates and Equivalent Isotropic Thermal Parameters (Å^2) for the Non-Hydrogen Atoms of $(Cu_2Br_2[(BVD)]_x)^a$

atom	x	y	z	U
Br	0.3798(2)	0.1427(3)	0.0	0.0577(7)
Cu	0.5	0.0	0.1812(2)	0.0558(8)
N1	0.6114(7)	0.3340(14)	0.3706(10)	0.043(3)
N2	0.5549(7)	0.1664(14)	0.3690(10)	0.038(3)
C3	0.5321(12)	0.097(2)	0.5	0.036(5)
C9	0.6476(12)	0.416(2)	0.2248(14)	0.067(5)
O1	0.6963(11)	0.577(2)	0.5	0.061(5)
C2	0.6461(12)	0.428(3)	0.5	0.036(5)

[a] For anisotropic atoms, the U value is U_{eq}, calculated as $U_{eq} = (1/3)\sum_i\sum_j U_{ij}a_ia_jA_{ij}$ where A_{ij} is the dot product of the ith and jth direct space unit cell vectors.

cannot be obtained and, consequently, the value of the longitudinal relaxation time (T_1) cannot be measured in a straightforward manner. The transverse relaxation time (T_2) can, however, be determined by a line shape analysis.[16,17] In the polymers, this is simplified by the high density of spins. In a magnetically nondilute, paramagnetic crystal, efficient exchange between neighboring spin centers within the crystal lattice results in $T_1 \approx T_2$ and averages all hyperfine and fine structure to zero. The resulting absorption has a Lorentzian shape in the center

(16) Atsarkin, V. A.; Demidov, V. V.; Vasneva, G. A. *Phys. Rev. B* **1995**, *52*, 1290.

(17) Atsarkin, V. A.; Vasneva, G. A.; Demidov, V. V. *JETP* **1995**, *81*, 509.

Table 4. Bond Lengths (Å) and Angles (deg) for the Non-Hydrogen Atoms of $(Cu_2Br_2[(BVD)]_x)^a$

1	2	3	1−2	1−2−3
Cu	Br	Cu′	2.410(2)	83.13(9)
Br	Cu	Br′		96.87(9)
N2	Cu	Br	2.118(9)	121.0(2)
N2	Cu	Br′		121.5(2)
N2	Cu	N2B		77.1(5)
N2	N1	C9	1.338(13)	118.3(9)
C9	N1	C2	1.47(2)	116.9(10)
C2	N1	N2	1.378(13)	124.6(9)
C3	N2	Cu	1.281(11)	115.9(9)
C3	N2	N1		114.9(10)
Cu	N2	N1		129.2(7)
C3B	C3	N2	1.54(3)	115.5(8)
N2A	C3	N2		128.9(15)
O1	C2	N1	1.19(2)	124.0(7)
N1	C2	N1A		111.9(15)

[a] Atoms labeled by primes are related by $1 - x, -y, -z$. Those atoms labeled by A are related by $x, y, 1 - z$, while those labeled by B are related by $1 - x, -y, z$ (see Figure 3).

with a line width determined by T_2 according to[18]

$$T_2 = \frac{2}{\sqrt{3}}\frac{1}{\gamma\Delta B_{pp}}$$

where γ is the magnetogyric ratio for the electron and ΔB_{pp} is the peak-to-peak line width measured from the first derivative of the absorption curve. In the wings of the spectrum, the line shape is expected to deviate from Lorentzian at a point roughly proportional to the magnitude of the exchange.[18] In our complexes, where the exchange rate is very high, deviation from Lorentzian behavior occurs only in the very extreme wings of the spectrum and is difficult to observe. This feature also makes moment analysis risky, so that measurement of the moments of the lines will add little to the analysis. T_2 for the polymeric species investigated is plotted as a function of temperature in Figure 6.

Molar magnetic susceptibility was recorded for all three samples from 1.7 to 350 K (Figure 7). The broad maximum in the susceptibility indicates that antiferromagnetic exchange predominates in all three complexes and that the interactions are largely one-dimensional. At low temperatures, a reciprocal temperature dependence (Curie law dependence) indicates the presence of doublet radical impurities. The poor approximation of these data by the Bleaney−Bowers equation for susceptibility

(18) Anderson, P. W.; Weiss, P. R. *Rev. Mod. Phys.* **1953**, *25*, 269.

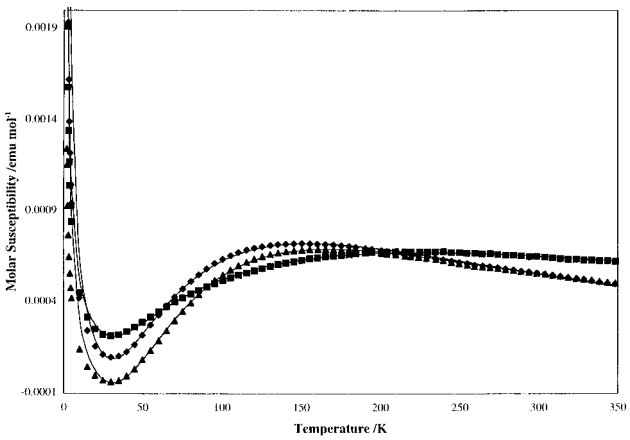

Figure 7. Temperature dependence of magnetic susceptibility for $[Cu_2Cl_2(BVD)]_x$ (diamonds), $[Cu_2Br_2(BVD)]_x$ (triangles), and $[Cu_2I_2(BVD)]_x$ (squares). The solid lines are best fits to the modified Barnes−Riera equation described in the text, with parameters $J_1 = -190$ cm^{-1}, $J_2 = -116$ cm^{-1}, $\chi_{dia} = -0.00029$ emu/mol, and $C = 0.009$ (emu K)/mol, ($[Cu_2Cl_2(BVD)]_x$); $J_1 = -200$ cm^{-1}, $J_2 = -110$ cm^{-1}, $\chi_{dia} = -0.00026$ emu/mol, and $C = 0.006$ (emu K)/mol ($[Cu_2Br_2(BVD)]_x$), and $J_1 = -271$ cm^{-1}, $J_2 = -200$ cm^{-1}, $\chi_{dia} = 2.3 \times 10^{-5}$ emu/mol, and $C = 0.005$ (emu K)/mol, ($[Cu_2I_2(BVD)]_x$).

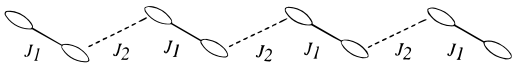

Figure 8. Exchange interactions in the alternating one-dimensional Heisenberg model. The ellipses represent individual verdazyl rings.

of isolated dimers indicates that exchange interactions between diradicals are important.

Inspection of the molecular packing diagram reveals a probable pathway for magnetic exchange interactions: namely, exchange between the two halves of the bis(verdazyl) π system and exchange across the π stack between polymer chains. Exchange across the copper−halide−copper bridges is assumed to be small relative to the other exchange parameters and is ignored. (Measurement of interaction between imino nitroxide radicals across a similar copper halide bridge gave an exchange constant of 2.2 cm^{-1}.[19]) The above interactions suggest that the observed magnetic susceptibility should be modeled as an alternating Heisenberg chain; that is, the exchange can be modeled using two exchange constants that alternate between magnetic centers along a one-dimensional chain (Figure 8). This model has the spin Hamiltonian:

$$\hat{H} = -\sum_{i}^{n/2}(J_1\mathbf{S}_{2i}\cdot\mathbf{S}_{2i+1} + J_2\mathbf{S}_{2i}\cdot\mathbf{S}_{2i-1})$$

Approximate equations for the temperature dependence of the susceptibility of this system have been developed by Hatfield[20] and by Barnes and Riera.[21] This model accurately describes the temperature dependence of the susceptibility for all three compounds (Figure 7). Best fit parameters obtained by least squares minimization for both models are $J_1 = -190$ cm^{-1} and $J_2 = -116$ cm^{-1} for $[Cu_2Cl_2(BVD)]_x$, $J_1 = -200$ cm^{-1} and $J_2 = -110$ cm^{-1} for $[Cu_2Br_2(BVD)]_x$, and $J_1 = -271$ cm^{-1} and $J_2 = -200$ cm^{-1} for $[Cu_2I_2(BVD)]_x$. If the exchange within the bis(verdazyl) molecule can be assumed to be only weakly dependent on the auxiliary copper ligands, we can assign the intraligand exchange to the values closest to the singlet−triplet splitting observed for the solution species **1**. This gives, for the intraligand exchange, $J_{intra} = -190$ cm^{-1} for the CuCl complex, $J_{intra} = -200$ cm^{-1} for the CuBr complex, and $J_{intra} = -200$ cm^{-1} for the CuI complex. The intermolecular exchange is similar for the CuCl and CuBr complexes (110 and 116 cm^{-1}) since they are isomorphic, but that for the CuI complex is strikingly different (271 cm^{-1}) as a result of differences in molecular packing.

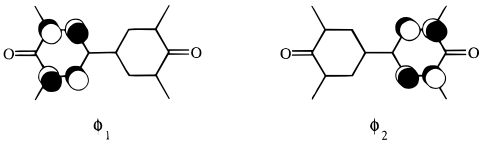

Figure 9. A cartoon representation of localized magnetic orbitals for the diradical BVD. Symmetric and antisymmetric combination of these orbitals gives rise to the singlet ground state and triplet excited state of BVD, respectively.

Discussion

Coordination of copper to the bis(verdazyl) ring system results in significant perturbation of the electronic structure of this diradical. In the three polymeric complexes, and in the monomeric solution species, the lowest excited triplet state is considerably stabilized compared with the free ligand. The ESR spectra are also indicative of an unusual electronic structure. Extremely fast spin relaxation in the solid phase is usually characteristic of certain transition metal electronic configurations (such as d^2V(III) and d^7-Co(II)) as a result of interaction with a low-lying excited state. Such short relaxation times are quite rare for organic species in rigid media.[22]

The unusual properties of this series of complexes can be understood by considering the interactions of the copper d orbitals with the molecular orbitals of the verdazyl system. We first discuss possible descriptions of the ligand orbitals. A detailed investigation of the ligand has already been made.[7] We begin our discussion at the Hückel level. While this approach is undoubtedly simplistic, the Hückel model and similar one-electron methods provide a relatively useful base for discussing further magnetic interactions.[23,24] Use of a somewhat more sophisticated semiempirical calculation (such as AM1) results in essentially the same singly occupied orbitals for the verdazyl and a qualitatively similar result. Conversely, accurate determination of the energies of the ground and excited states of these systems requires lengthy calculation.[25]

At the Hückel level (i.e., including only nearest neighbor interactions), there are two degenerate highest occupied orbitals, each containing one electron. While these orbitals can be drawn as delocalized over the entire ligand π system, it is more convenient to use localized orbitals, one on each verdazyl system. Such a description is defensible at this level because of the disjoint nature of the bis(verdazyl) system. A cartoon depicting these localized orbitals, ϕ_1 and ϕ_2, is shown in Figure 9. Such singly occupied orbitals have been labeled "natural magnetic orbitals" by Kahn.[4] As described by Kahn, and also by Auerbach,[26] the exchange energy between the electrons in such orbitals depends on orbital overlap and the proximity of the orbitals to each other in space. Overlap between the orbitals

(19) Oshio, H.; Watanabe, T.; Ohto, A.; Ito, T.; Masuda, H. *Inorg. Chem.* **1996**, *35*, 472.
(20) Hatfield, W. E. *J. Appl. Phys.* **1981**, *52*, 1985.
(21) Barnes, T.; Riera, J. *Phys. Rev. B* **1994**, *50*, 6817.
(22) Bertini, I.; Martini, G.; Luchinat, C. In *Handbook of Electron Spin Resonance;* Poole, C. P. J., Farach, H. A., Eds.; AIP Press: New York, 1994; p 79.
(23) Miller, J. S.; Epstein, A. J. *Angew. Chem., Int. Ed. Engl.* **1994**, *33*, 385.
(24) Miller, J. S.; Epstein, A. J. *Chem. Eng. News* **1995**, *73*, 30.
(25) Nachtigall, P.; Jordan, K. D. *J. Am. Chem. Soc.* **1993**, *115*, 270.
(26) Auerbach, A. *Interacting Electrons and Quantum Magnetism;* Springer-Verlag: New York, 1994.

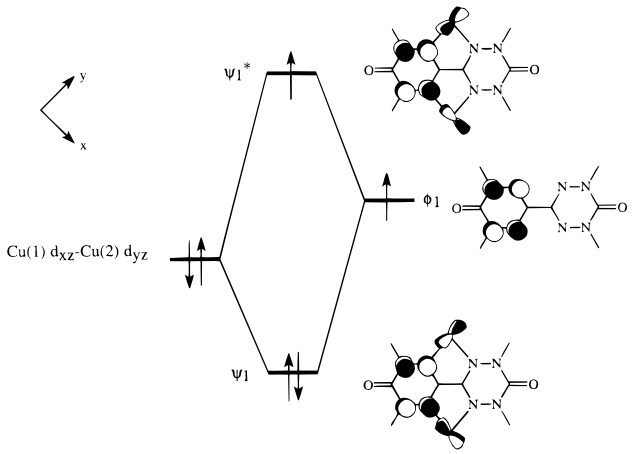

Figure 10. Interaction of BVD singly occupied orbitals (natural magnetic orbitals) with copper d orbitals. Overlap of the copper d orbital with BVD SOMOs results in significant spin density on copper, enhancing the effects of electron−electron repulsion and lowering the energy of the triplet state.

tends to result in spin-pairing, minimizing the electron kinetic energy and stabilizing the singlet state. Close proximity of the orbitals instead favors the triplet state as a result of minimization of electron−electron repulsion. In the isolated diradical, long-range overlap between verdazyl SOMOs results in a weak bonding interaction, while electron repulsion is minimized as a result of the localized nature of the orbitals. The result is that the ligand diradical has a singlet ground state with the triplet lying 760 cm^{-1} above it.[7]

The preferential formation of the copper(I) complex from either copper(I) or copper(II) halides suggests that, like the related aromatic imines, the bis(verdazyl) ligand is a relatively strong π acceptor. As a result, there is significant overlap between the metal d orbitals and the ligand π system; thus, the copper−nitrogen bond has significant dπ−pπ character. A similar situation is observed in the radical cation **3**.[27,28] In this

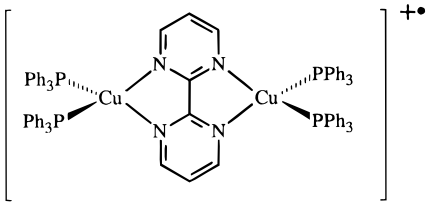

3

cation, which is formally a copper (I) complex of the 2,2′-bipyrimidine radical anion, ESR hyperfine coupling indicates that the unpaired electron is delocalized over both the 2,2′-bipyrimidine ligand and the copper atoms.

Returning to the individual verdazyl SOMOs and the natural magnetic orbital scheme discussed above, we see that overlap of ϕ_1 with copper d_{xz} and d_{yz} orbitals results in the orbitals ψ_1 and ψ_1* depicted in Figure 10. Similarly ϕ_2 will give rise to a similar pair of orbitals ψ_2 and ψ_2*. Although there is still no net overlap between the magnetic orbitals ψ_1* and ψ_2* on nearest neighbors (since the relevant copper d orbitals involved are orthogonal), they can no longer be confined to separate groups of atoms. The resulting Coulombic repulsion between the electrons stabilizes the triplet state, resulting in the reduced exchange interactions seen in the copper complexes.

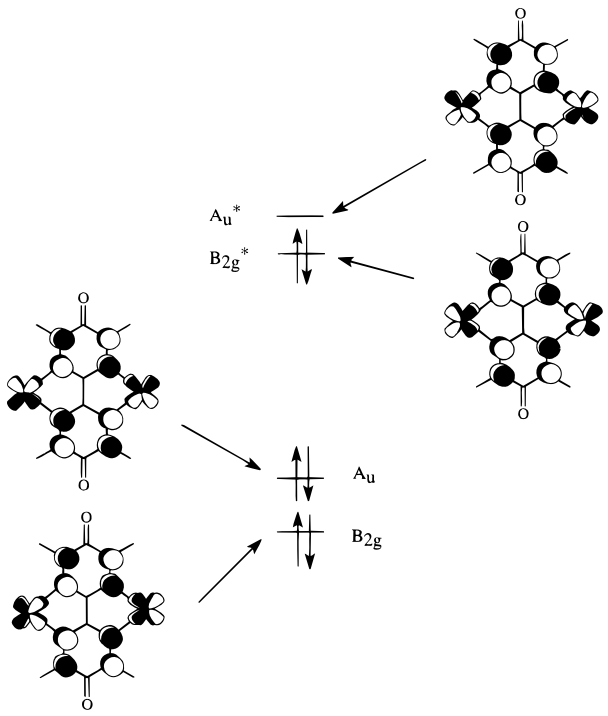

Figure 11. Qualitative orbital scheme for interaction of Cu(I) with BVD.

It is convenient to consider this model as a competition between a direct exchange pathway favoring a singlet ground state and a superexchange pathway through the copper atoms favoring a triplet ground state. A qualitative molecular orbital scheme depicting the interaction of the highest energy ligand π and metal d orbitals is shown in Figure 11. The A_u and B_{2g} levels result from symmetric and antisymmetric combination of the orbitals ψ_1 and ψ_2. Similarly, the A_u* and B_{2g}* levels arise from combination of ψ_1* and ψ_2*.

In the case of the copper complexes of BVD, this exchange mechanism is effective. Although the ground state is still a singlet, the stabilization of the bis(verdazyl) triplet state as a result of coordination of the copper atoms is about 500 cm^{-1}. By comparison, exchange between imino nitroxide ligands mediated by tetrahedral copper(I) is ferromagnetic with $J =$ 100 cm^{-1} [29] and the magnitude of the exchange interaction between semiquinone ligands mediated by diamagnetic metal centers is on the order of 5−40 cm^{-1}.[30] This considerably weaker interaction is a result of the localized nature of semiquinone SOMOs in metal complexes.[6] With little unpaired electron density on the metal atom, the contribution of the superexchange mechanism is diminished. When the orbital match is improved (for instance, in superexchange between copper(II) centers mediated by a 2,2′-bipyrimidine ligand), the strength of the interaction is increased.[31] To achieve strong interactions, whether ferromagnetic or antiferromagnetic, a close match of the respective orbitals is required such that unpaired electron density is delocalized between the metal and ligand. In $[Cu_2X_2(BVD)]_x$, the ligand and metal orbitals are close enough in energy, and have the appropriate symmetry, to produce a large ferromagnetic exchange.

We can use this model to make rough predictions concerning the magnitude of the superexchange interaction. The interac-

(27) Vogler, C.; Hausen, H. D.; Kaim, W.; Kohlmann, S.; Kramer, H. E.; Rieker, J. *Angew. Chem., Int. Ed. Engl.* **1989**, *28*, 13659.
(28) Vogler, C.; Kaim, W.; Hausen, H.-D. *Z. Naturforsch.* **1993**, *48b*, 1470.
(29) Oshio, H.; Watanabe, T.; Ohto, A.; Ito, T.; Nagashima, U. *Angew. Chem., Int. Ed. Engl.* **1994**, *33*, 670.
(30) Lange, C. W.; Conklin, B. J.; Pierpont, C. G. *Inorg. Chem.* **1994**, *33*, 1276.
(31) Castro, I.; Sletten, J.; Glærum, L. K.; Lloret, F.; Faus, J.; Julve, M. *J. Chem. Soc., Dalton Trans.* **1994**, 2777.

tions illustrated in Figures 9 and 10 suggest that the degree of triplet stabilization will depend on the unpaired electron density on the copper atom and, hence, on the extent of Cu−N π bonding. Auxiliary copper ligands that increase d-orbital participation in this π bonding would increase the stabilization of the triplet over that of the singlet state. Conversely, strong π acceptor ligands would reduce the degree of copper−BVD π bonding and would stabilize the singlet state. Since the proposed orbital interaction imparts some copper(II) character to the metal center, the ligands best able to stabilize the higher oxidation state would give rise to a greater triplet stabilization. It does appear that the intramolecular exchange with the chloride complex is slightly lower than that with iodide or bromide, but the trend is weak. The trend among the halides is better revealed in the ESR spectra. Trimethyl phosphite, however, is a strong π acceptor, reducing the degree of Cu−N π bonding in the monomer **1** and destabilizing the triplet state by 30 cm^{-1}.

To gain further insight into the copper−verdazyl interaction, we can look at the ESR data. Unlike the magnetic data, the spin relaxation rate is very sensitive to the copper auxiliary ligands, with the ligands better able to stabilize copper(II), producing a faster relaxation rate. This suggests that the relaxation is related to the spin density on the copper atoms, and an understanding of the relaxation mechanism should lead to greater understanding of the complex's electronic structure.

The observed relaxation rate is unusually fast for an organic radical (T_2 for an organic radical is typically 10^{-6} s[22]), and inspection of Figure 1 indicates that it is considerably faster than the relaxation in the isolated BVD ligand. The similarity of the relaxation rates for the solution species and the polymers suggests a common relaxation mechanism. The weak temperature dependence indicates that the relaxation does not occur through a standard Orbach or Raman process.[32] In fact, weak or no temperature dependence is typical for strongly exchange-coupled lattices.[15,33,34]

Two possible cases can be envisioned depending upon the nature of the solution species. If the solution species is predominantly dimeric (**2**) or oligomeric, spin relaxation probably results from interaction between neighboring triplets across the halide bridge. (A similar mechanism was proposed to account for the temperature dependent relaxation observed in the dimeric copper acetate−pyrazine complex ($Cu_2Ac_4(pyz)$).[35]) The temperature dependence of this relaxation will vary with the probability of the neighboring verdazyl unit being in the triplet state. In $Cu_2Ac_4(pyz)$, such dependence was used to determine the magnitude of the exchange between triplets.[35] Unfortunately, because the determination of line width for our solution species is so crude, a meaningful quantitative fit of the data is impossible. For the solid state, because J_2/J_1 is large, the concept of isolated triplets is inappropriate and application of the theory more complicated. Nevertheless, we might expect the reciprocal of the relaxation rate to follow the product of susceptibility and temperature (χT) and be strongly dependent on the identity of the halide. Halides that increase the spin density on copper would increase the facility of exchange across the halide bridge and produce faster relaxation times. The observed data are qualitatively consistent with this model; however, a full analysis requires single-crystal ESR data, measured over a greater temperature range. Such data are currently unavailable because of the lack of suitable single crystals for the iodide complex and because of the partial instability of the complex in solution over long periods.

Alternatively, if the species in chloroform solution is predominantly a monomer (**1**), the very rapid spin relaxation must be a result of the copper−verdazyl interaction itself. As previously noted, such short relaxation times are usually associated with transition metal ions having low-lying spin states that can interact with the ground state. A similar mechanism working on a molecular scale could account for the fast relaxation in the copper−bis(verdazyl) system. In this case, rapid spin relaxation may result from interaction between the first excited triplet state and a higher triplet state. A possible candidate for this higher energy electronic state is the triplet "metal-to-ligand charge transfer" (^{3}MLCT) state which has been found to be characteristic of copper(I) complexes of chelating aromatic imines.[11,36] This state is typically low in energy and has been detected from its phosphoresence in the red and near-IR spectral regions,[11,36] although no phosphorescence was detected from **1**. In the context of Figure 10, this state corresponds to half-filled A_u and A_u* orbitals. Increased metal-to-ligand π bonding would lower the energy of this triplet as a result of the greater electron−electron repulsion associated with increased delocalization. A lower energy triplet would lead to greater triplet−triplet interaction and increased line broadening. Thus, a spin relaxation mechanism involving a higher energy electronic state is fully consistent with the auxiliary ligand dependence of the ESR line width.

Although strongly exchange-coupled lattices have relaxation times relatively independent of temperature, the monomer should also have a strongly temperature dependent relaxation time, which in turn could be used to determine the energy of the excited state responsible for the relaxation. The line width of the solution species is, in fact, temperature dependent, but the errors involved in its accurate determination prevent a truly meaningful analysis.

Thus, both relaxation models are consistent with our description of the electronic structure, and currently available data do not enable us to distinguish unambiguously between them. Further understanding of these unusual systems will result from a detailed study of the temperature and orientational dependence of the line shape in a well-characterized, monomeric verdazyl complex.

Conclusions

The reaction of copper halides with 1,1′,5,5′-tetramethyl-6,6′-dioxobis(verdazyl) results in a new series of coordination polymers. Although the intraligand electronic exchange is still antiferromagnetic in these systems, the triplet excited state is considerably stabilized compared with the free ligand as a result of an increasingly important superexchange through the copper(I) center. The strength of this exchange is probably a result of the close matching of the energies of the ligand π and metal d orbitals, and initial results suggest that the interaction may be tuned by careful consideration of the copper auxiliary ligands. The bridging ability of the BVD ligand lends itself to the formation of extended coordination polymers and holds promise for other new and exciting magnetic systems.

Experimental Section

General Procedures. ESR spectra were recorded on a Bruker ESP300 ESR spectrometer equipped with an E4100 variable temperature controller. X-ray powder patterns were recorded on a Phillips

(32) Standley, K. J.; Vaughan, R. A. *Relaxation Phenomena in Solids;* Plenum Press: New York, 1969.

(33) Richards, P. M. In *Local Properties at Phase Transitions;* Müller, K. A., Rigamonti, A., Eds.; North-Holland: Amsterdam, 1976.

(34) Bencini, A.; Gatteschi, D. *EPR of Exchange Coupled Systems;* Springer-Verlag: New York, 1990.

(35) Valentine, J. S.; Silverstein, A. J.; Soos, Z. G. *J. Am. Chem. Soc.* **1974**, *96*, 97.

(36) Everly, R. M.; McMillin, D. R. *J. Phys. Chem.* **1991**, *95*, 9071.

automated diffractometer equipped with a graphite monochromator using Cu Kα radiation. Powder patterns were indexed and unit cell parameters refined with the programs TREOR and VISSER as implemented in the software package PROSZKI.[14] Absorption spectra were recorded with a Hewlett-Packard HP-8452 diode array spectrometer. Infrared spectra were recorded with a Perkin-Elmer Model 1600 or a Nicolet 510P Fourier transform infrared spectrometer. Copper(II) chloride dihydrate, copper(II) bromide, copper(I) chloride (99.995% pure), copper(I) bromide (99.999% pure), copper(I) iodide, and trimethyl phosphite−copper(I) iodide (Aldrich) were used as received.

Because of the extreme insolubility of the polymeric complexes, the samples were difficult to obtain rigorously pure, and consequently results of elemental analyses were unsatisfactory. Nevertheless, only lines consistent with the reported unit cells were observed in X-ray powder diffraction measurements.

Magnetic Measurements. Magnetic susceptibilities were measured on a Quantum Design MPMS-5 SQUID magnetometer. Data were collected on powdered samples over a 1.7−350 K temperature range at a field of 5000 G. Data were corrected for the diamagnetism of the sample holder. Data between 20 and 350 K were fitted to the equation

$$\chi = \chi_{spin}(J_1,J_2,T) + \chi_{dia} + C/T$$

where $\chi_{spin}(J_1,J_2,T)$ is the function described by Barnes and Riera[21] for an alternating Heisenberg chain, χ_{dia} is the sample diamagnetism, and C/T is the Curie susceptibility of the paramagnetic impurity. Best-fit curves were obtained using a least-squares method with both exchange constants, the sample diamagnetism, and the amount of impurity as fitted parameters. This gave the exchange parameters reported above and, for the CuCl complex, $\chi_{dia} = -0.00029$ emu/mol and $C = 0.009$ (emu K)/mol, for the CuBr complex, $\chi_{dia} = -0.00026$ emu/mol and $C = 0.006$ (emu K)/mol, and, for the CuI complex, $\chi_{dia} = 2.3 \times 10^{-5}$ emu/mol and $C = 0.005$ (emu K)/mol. These values are consistent with the presence of 1−2% of paramagnetic impurity.

Reaction of BVD with Trimethyl Phosphite−Copper(I) Iodide. Nitrogen-purged chloroform (0.5 mL), BVD (10 mg), and $(CH_3O)_3$PCuI (20 mg) were combined in an ESR tube. The tube was shaken to mix the reagents, and then the ESR spectrum of the frozen solution was recorded at temperatures from 110 to 200 K. The product of relative integrated intensity and temperature was fitted to the modified Bleany−Bowers equation

$$IT = q/(3 + e^{-J/k_BT}) + p$$

with parameters $J = -230$ cm^{-1}, $q = 8.1$ K, and $p = 0.17$ K. An IR spectrum of this solution was also recorded giving $\nu_{CO} = 1697$ cm^{-1}.

Alternatively, 3.55 mg of BVD was dissolved in 25 mL of dichloromethane. To this solution was added 12.71 mg of $(CH_3O)_3$PCuI, and the mixture was shaken vigorously. UV−vis spectroscopy gave $\lambda_{max} = 396$ nm with $\epsilon = 4700$ L mol^{-1} cm^{-1}. A long featureless tail extended from 396 to 750 nm.

Cu_2Cl_2(BVD). Method a. A solution of 50 mg (0.2 mmol) of BVD in 2 mL of chloroform was combined with a solution of 68 mg (0.4 mmol) of copper(II) chloride dihydrate in 2 mL of methanol. Having been stirred for 24 h, the resulting black microcrystalline precipitate was removed by filtration to give 65 mg (72%) of $[Cu_2Cl_2(BVD)]_x$ with IR (KBr) 1699 cm^{-1}. A finely powdered sample was used for X-ray powder diffraction. Indexing of the powder pattern gave an orthorhombic cell with dimensions $a = 6.684$ Å, $b = 12.524$ Å, and $c = 8.717$ Å.

Cu_2Cl_2(BVD). Method b. A solution of 104 mg of BVD in 2 mL of chloroform was combined with an argon-purged solution of 82 mg of CuCl in 2 mL of acetonitrile. A black precipitate began to form immediately. Having been stirred for 24 h, the precipitate was collected by filtration to give 157 mg (84%) of Cu_2Cl_2(BVD). The infrared spectrum and X-ray powder pattern were identical to those of the sample prepared by method a.

Cu_2Br_2(BVD). Method a. A solution of 90 mg of anhydrous copper(II) bromide in methanol was carefully layered onto a solution of 50 mg of BVD in chloroform. The two layers were allowed to diffuse together over a 48 h period. Filtration gave a black crystalline precipitate of Cu_2Br_2(BVD) with an IR band (KBr) at 1695 cm^{-1} (C═O). The crystals grew as very thin, black plates with rounded faces. A data crystal was selected with approximate dimensions 0.05 × 0.19 × 0.39 mm. The data were collected at −75 °C on a Siemens P3 diffractometer using a graphite monochromator with Mo Kα radiation ($\lambda = 0.710\,73$Å). Details of crystal data, data collection, and structure solution and refinement are listed in Table 2. Four reflections (−1, −1, 2; −1, 0, −3; 1, 1, −2; 1, 1, 2) were remeasured every 96 reflections to monitor instrument and crystal stability. A smoothed curve of the intensities of these check reflections was used to scale the data. The scaling factor ranged from 0.9691 to 1.007. The data were corrected for *Lp* effects and absorption. The absorption correction was based on crystal shape measurements with minimum and maximum transmission factors ranging from 0.2271 to 0.5118. Data reduction, decay and absorption correction, and structure solution and refinement were performed using the SHELXTL-Plus software package.[37] The structure was solved by direct methods and refined by full-matrix least-squares on F^2 with anisotropic thermal parameters for the non-H atoms. The hydrogen atoms on the methyl carbon, C9, were calculated in idealized positions (C−H 0.98 Å) with isotropic temperature factors set to $1.5U_{eq}$ of C9. The function $\sum w(|F_o|^2 - |F_c|^2)^2$ was minimized, where $w = 1/[(\sigma(F_o))^2 + (0.08P)^2]$ and $P = (|F_o|^2 + 2|F_c|^2)/3$. Neutral atom scattering factors and values used to calculate the linear absorption coefficient are from the *International Tables for X-ray Crystallography* (1990).[38] Other computer programs used in this work are listed elsewhere.[39] All crystallographic figures were generated using XP/PC.[40]

Cu_2Br_2(BVD). Method b. To a 99 mg sample of BVD dissolved in 2 mL of nitrogen-purged chloroform was added a solution of 113 mg of copper(I) bromide in 2 mL of nitrogen-purged acetonitrile. The solution was allowed to stand at room temperature for 15 h, and the precipitate of 164 mg (77%) of Cu_2Br_2(BVD) was removed by filtration and dried under vacuum.

Cu_2I_2(BVD). A solution of 76 mg of copper(I) iodide in 4 mL of nitrogen-purged acetonitrile was combined with a solution of 50 mg of BVD in 2 mL of nitrogen-purged chloroform. After the solution was allowed to stand for 24 h, filtration gave a black microcrystalline precipitate of 82 mg (65%) of Cu_2I_2(BVD). This material had an IR band (KBr) at 1707 cm^{-1} (C═O). X-ray powder diffraction data were collected on a finely powdered sample. Indexing of the powder pattern gave a monoclinic unit cell with dimensions $a = 12.669$ Å, $b = 8.461$ Å, $c = 7.679$ Å, and $\beta = 91.88°$.

Acknowledgment. We thank Ron Goldfarb and NIST for the use of the SQUID magnetometer, Professor Tad H. Koch for allowing the continuation of this work in his laboratories, and Professor Cortlandt Pierpont for helpful discussions. Funding was provided by the National Science Foundation and the Robert A. Welch Foundation.

Supporting Information Available: Tables giving the anisotropic and isotropic thermal parameters, fractional coordinates, bond lengths and angles, and torsion angles for $(Cu_2Br_2[(BVD)]_x$ (4 pages). See any current masthead page for ordering and Internet access instructions.

JA961675Y

(37) Sheldrick, G. M. *SHELXTL-PLUS*, Version 5.03; Siemens Analytical X-ray Instruments, Inc.: Madison, 1994.

(38) Wilson, J. C., Ed. *International Tables for X-ray Crystallography*; Kluwer Academic Press: Boston, 1992; Vol. C, Tables 4.2.6.8 and 6.1.1.4, A.

(39) Gadol, S. M.; Davies, R. E. *Organometallics* **1982**, *1*, 1607.

(40) *XP/PC*, V 5.03; Siemens Analytical X-ray Instruments, Inc.: Madison, 1994.